Original Article

Association of vulnerable plaques with white matter hyperintensities on high-resolution magnetic resonance imaging

Jiayu Li[1#], Yuan Tian[1#], Ying Shi[1], Yingzhe Cui[1], Jianxiu Lian[2], Pengfei Liu[1]

[1]Department of Magnetic Resonance, the First Affiliated Hospital of Harbin Medical University, Harbin, China; [2]Philips Healthcare, Beijing, China

Contributions: Conception and design: J Li, P Liu; (II) Administrative support: P Liu, Y Cui; (III) Provision of study materials or patients: All authors; (IV) Collection and assembly of data: J Li, Y Tian; (V) Data analysis and interpretation: All authors; (VI) Manuscript writing: All authors; (VII) Final approval of manuscript: All authors.

[#]These authors contributed equally to this work.

Correspondence to: Pengfei Liu, PhD. Department of Magnetic Resonance, the First Affiliated Hospital of Harbin Medical University, 1st Floor, 3#Building, No. 23, Youzheng Street, Nangang District, Harbin 150001, China. Email: liup.fei@163.com.

Background: One of the widespread manifestations of cerebral small vessel disease (CSVD) of the brain parenchyma is white matter lesion, which appears as white matter hyperintensities (WMHs) on magnetic resonance imaging (MRI). Previous studies have illustrated that large artery atherosclerosis is related to CSVD, but the precise progress of pathogenesis remains unknown. High-resolution MRI (HR-MRI) has the ability to delineate intracranial vascular walls, enabling a thorough exploration of the structure and composition of unstable plaques. This study aimed to apply HR-MRI to characterize the wall changes and plaque characteristics of middle cerebral arteries in patients with WMHs and to investigate the correlation between plaque vulnerability parameters and different degrees of WMHs.

Methods: In this study, 138 patients with acute ischemic stroke at Harbin Medical University's First Clinical Hospital (May 2021 to October 2023) were cross-sectionally reviewed and underwent conventional brain and HR-MRI using T1-weighted 3D volumetric isotropic turbo spin echo acquisition (T1W-3D-VISTA) of the unilateral middle cerebral artery (MCA). According to Fazekas grade (0–6), the patients were divided into two groups: Fazekas score 0–2, no-or-mild WMHs; and Fazekas 3–6, moderate-to-severe WMHs. The intraplaque hemorrhage, plaque distribution, plaque enhancement, plaque load, remodeling pattern, and stenosis of the two groups were measured. Binary logistic regression analysis was conducted to evaluate the relationship between vulnerable plaques and WMHs.

Results: Of the participants who were initially considered for inclusion, 71 were deemed eligible, among whom 34 were placed in the no-or-mild WMH group and 37 in the moderate-to-severe WMH group. Between the two groups, there were significant differences in intraplaque hemorrhage (P=0.01), a wide distribution (P=0.02), and plaque enhancement (P=0.02). Univariate analysis showed that WMHs were associated with age [odds ratio (OR) =1.080; 95% confidence interval (CI): 1.020–1.144; P=0.008], hypertension (OR =3.500; 95% CI: 1.276–9.597; P=0.01), intraplaque hemorrhage (OR =3.955; 95% CI: 1.247–12.538; P=0.02), a wide distribution (OR =3.067; 95% CI: 1.159–8.115; P=0.02), and significant plaque enhancement (OR =4.372; 95% CI: 1.101–17.358; P=0.03); however, the multivariate results showed that the only independent factors associated with WMHs were age (OR =1.095; 95% CI: 1.019–1.176; P=0.01) and intraplaque hemorrhage (OR =5.88; 95% CI: 1.466–23.592; P=0.01).

Conclusions: Our findings suggest that age and intraplaque hemorrhage may be associated with more severe WMHs in patients with acute ischemic stroke, which may be helpful for further clinical examination and intervention treatment.

Keywords: Cerebral small vessel disease (CSVD); white matter hyperintensities (WMHs); atherosclerosis; magnetic resonance imaging (MRI); vulnerable plaque

Submitted Dec 28, 2023. Accepted for publication Mar 21, 2024. Published online Apr 26, 2024.
doi: 10.21037/qims-23-1856
View this article at: https://dx.doi.org/10.21037/qims-23-1856

Introduction

Cerebral small vessel disease (CSVD) is a common disease, particularly in older adults, and has received considerable attention in recent years. The modification of small blood vessels in the brain, influenced by an intricate interplay of factors, is closely associated with conditions such as ischemic stroke, dementia, and depression (1,2). Although the etiology of CSVD is unclear, it is known that the large and small cerebral blood vessels intertwine with each other to form a vascular network, which is morphologically and structurally connected. This network, influenced by hemodynamics, functions in a coordinated manner and is collectively exposed to various vascular risk factors. Thus, CSVD may be associated with lesions in the large arteries (3). Atherosclerosis of the large arteries is a widely prevalent global affliction and a significant contributor to ischemic stroke (4). Using high-resolution magnetic resonance imaging (HR-MRI) facilitates the analysis of atherosclerotic plaque characteristics and vascular changes in large arteries (5,6) and has proven instrumental to characterizing the features of vulnerable plaques.

Investigating the relationship between atherosclerotic plaques in large cerebral arteries and the white matter hyperintensities (WMHs) associated with CSVD is a critical step in medical research (7,8). However, there is a dearth of in-depth studies analyzing the association of WMHs with intracranial large arteries or vulnerable atherosclerotic plaques. In the study of Berman *et al.*, ultrasound was used to measure internal carotid artery plaque strain, and higher plaque strain was found to be one of the characteristics of vulnerable plaques (9). Their results showed that the internal carotid artery strain was positively correlated WMHs, and it was suggested that examining unstable plaques may be more informative than examining arterial stenosis. Compared with ultrasound, HR-MRI can more intuitively measure large blood vessels in the brain and calculate more parameters of unstable plaque, which can further enrich the research on the relationship between plaque instability and WMHs. In turn, identifying the correlation between plaque vulnerability parameters and WMHs in intracranial large arteries may provide insights into the mechanism of WMH formation.

In this study, we innovated the use HR-MRI to analyze atherosclerotic plaque characteristics (intraplaque hemorrhage, plaque distribution, plaque enhancement) and vascular alterations in the middle cerebral artery (MCA) of patients with acute ischemic stroke in different WMH subgroups. In order to aid clinicians in the early diagnosis and treatment of CSVD, this study aimed to clarify the relationship between vulnerable plaques and WMHs, identify the independent risk factors affecting WMHs, and empirically establish a theory correlating WMHs and vulnerable plaques. We present this article in accordance with the STROBE reporting checklist (available at https://qims.amegroups.com/article/view/10.21037/qims-23-1856/rc).

Methods

Participants

We collected patients with acute ischemic stroke admitted to the First Affiliated Hospital of Harbin Medical University from May 2021 to October 2023 who were suspected of having MCA stenosis by neurologists via HR-MRI. The main inclusion criteria were (I) age ≥18 years; (II) the presence of plaque in the M1 segment of the unilateral MCA confirmed by HR-MRI; (III) diffusion-weighted imaging (DWI) consistent with acute infarct foci in the blood-supplying region of the MCA, with an interval of no more than 1 week between the DWI and the HR-MRI examination; and (IV) the presence of two or more atherosclerosis risk factors such as hypertension, diabetes mellitus, dyslipidemia, and smoking. Meanwhile, the exclusion criteria were (I) contraindications to HR-MRI or contrast allergy; (II) presence of intracranial infections, tumor occupancy, congenital dystrophy of the cerebral white matter, and other central nervous system demyelinating disorders; (III) presence of nonatherosclerotic vascular diseases such as moyamoya disease, vasculitis, and arterial

Table 1 HR-MRI protocol parameters

Parameter	3D-TOF-MRA	T1W-3D-VISTA	T2W-3D-VISTA	SNAP
TR (ms)	25	800	1800	11
TE (ms)	3.5	19	226	6.4
Thickness (mm)	0.6	0.6	0.6	0.6
Gap (mm)	–0.7	–0.3	–0.3	–0.3
FOV (mm × mm)	194×194	200×181	200×181	160×160
Matrix	276×276	332×300	332×302	268×196
Slices	120	133	133	133
NSA	1	1	1	1
Voxel (mm × mm)	0.7×0.7	0.6×0.6	0.6×0.6	0.6×0.6

HR-MRI, high-resolution magnetic resonance imaging; 3D-TOF-MRA, three-dimensional time-of-flight magnetic resonance angiography; T1W-3D-VISTA, T1-weighted three-dimensional volumetric isotropic turbo spin echo acquisition; T2W-3D-VISTA, T2-weighted three-dimensional volumetric isotropic turbo spin echo acquisition; SNAP, simultaneous noncontrast angiography and intraplaque hemorrhage; TR, time of repetition; TE, time of echo; FOV, field of view; NSA, number of signal average.

entrapment; (IV) a recent history of radiotherapy, hormone, or immunosuppressant treatment of the head; and (V) poor quality of the images preventing further analysis.

Clinical data collection

This study was conducted in accordance with the Declaration of Helsinki (as revised in 2013) and was approved by the institutional review board of the First Hospital of Harbin Medical University (No. 2023JS24). The requirement for individual consent for this retrospective analysis was waived. The basic clinical information and imaging data of the participants were collected, including age, gender, height, weight, hypertension, diabetes, dyslipidemia, history of smoking, and a history of stroke or transient ischemic attack (TIA). The diagnostic criteria for hypertension were systolic blood pressure ≥140 mmHg and/or diastolic blood pressure ≥90 mmHg or being on medication for hypertension; diabetes mellitus was defined as a fasting glucose level of ≥7.0 mmol/L or a nonfasting glucose level of ≥11.1 mmol/L or undergoing treatment for diabetes mellitus; dyslipidemia was defined as a total cholesterol level of >5.2 mmol/L or low-density cholesterol >3.4 mmol/L or taking lipid-lowering drugs (10,11).

MRI screening procedure

All participants underwent routine head MRI and HR-MRI with a 3.0 T Achieva MR scanner (Philips Healthcare, Best, Netherlands) with a 16-channel phased-array head and neck coil. The head MRI and HR-MRI scanning protocol was as follows: T2-weighted-fluid-attenuated inversion recovery (T2 FLAIR), three-dimensional time-of-flight magnetic resonance angiography (3D-TOF MRA), DWI, pre- and post-enhancement T1-weighted 3D volumetric isotropic turbo spin echo acquisition (T1W-3D-VISTA), T2W-3D-VISTA, and simultaneous noncontrast angiography and intraplaque hemorrhage imaging (SNAP). Magnetic resonance contrast was performed using gadobutrol (1.0 M; Gadovist; Bayer Schering Pharma, Berlin, Germany) at a rate of 4 mL/s, with a dosage of 0.1 mL/kg, which was followed by an additional 20 mL of saline at a rate of 2 mL/s. The T1W-3D-VISTA parameters were the same before and after enhancement. The scanning parameters are summarized in *Table 1*.

Image analysis

After image acquisition and transfer to an IntelliSpace Portal 10.1 workstation (Philips Healthcare) for postprocessing, qualitative and quantitative assessments of MRI imaging were completed by two neuroradiologists (PFL and YZC, each with 10 years of experience in neuroimaging) who were unaware of the clinical information of the participants. If the grading results were inconsistent, the two neuroradiologists discussed them until arriving to a consensus.

Image quality was graded into three levels: level 1—

the outer vessel and lumen could not be visualized; level 2—the outer vessel and lumen could be visualized, with a few areas of blurring that did not interfere with plaque characterization; and level 3—the wall and lumen edges were clear (12). Only image quality ≥ grade 2 could be included for subsequent image analysis.

For semiquantitative assessment, patients with WMHs were divided into two groups according to the modified Fazekas score (0–6) based on the T2 FLAIR-TRA imaging results (13). Those with a Fazekas score of 0–2 were placed into a no-or-mild WMH group (group 1), and those with a Fazekas score of 3–6 were placed into the moderate-to-severe WMH group (group 2). The modified Fazekas scoring criteria included a paraventricular high signal portion and a deep white matter portion (1). The scoring for a paraventricular high signal was determined as follows: 0, no lesion; 1, a cap-like or pencil-tip-like thin lesion; 2, a smooth halo of the lesion; and 3, an irregular paraventricular high signal extending into the deep white matter (2). Meanwhile, the scoring for deep white matter signal was determined as follows: 0, no lesion; 1, a punctate lesion; 2, incipient fusing of the lesion; and 3, a lesion fused over a large area. The scores of the two portions were added together to calculate the total score (14).

Narrow side plaque characteristics were analyzed independently via a double-blind method on HR-MRI by other two professional radiologists (Y.T. and Y.S., each with 5 years of experience in neuroimaging) who selected cross-sectional images of the arterial vessels. If there was a disagreement regarding the classification, the two radiologists arrived at a consensus after discussion. For determining the presence or absence of intraplaque hemorrhage, intraplaque hemorrhage was considered present when there were areas of high signal (>150% of the adjacent area of the vessel wall) within the plaque on the T1W-3D-VISTA images, with short bars and punctate high signals in the corresponding locations on the SNAP sequence (15). Plaque enhancement was categorized into grades 0–2 as follows: grade 0, enhancement below or close to the normal intracranial artery wall; grade 1, enhancement greater than grade 0 but lower than the pituitary signal; and grade 2, enhancement similar to or higher than that of the pituitary (16). We defined grade 0–1 enhancement as nonsignificant and grade 2 as significant. The distribution of plaque location was evaluated at the level of maximum stenosis of the vessel, and the short-axis position of the MCA was categorized into superior, inferior, ventral, or dorsal sidewalls. The plaque was considered to be wide when it was distributed in two or more vessel sidewalls; otherwise, it was categorized as limited (17).

Quantitative parameters were determined by two radiologists by outlining the region of interest (ROI) after fourfold magnification on the enhanced T1W-3D-VISTA images, with the internal ROI being the interface between the vessel wall lining and the blood and the external ROI being the interface between the outer wall of the vessel and the cerebrospinal fluid. Plaque load was quantified by a standardized wall index, in which the stenotic vessels were selected at the level of the largest plaque, and the reference vessels were selected by visual assessment; preference was given to proximal normal vessels with the wall at the level of the largest stenosis and then to distal normal vessels. Based on the ROI, the vessel area at the stenosis level (VA stenosis), the lumen area (LA stenosis), the vessel area at the reference level (VA reference), and the lumen area (LA reference) were recorded. Based on the measured values, the degree of stenosis, remodeling index, and plaque load were calculated. The formulas for calculating the relevant parameters were as follows: standardized wall index = (1 – LA stenosis/VA stenosis) × 100% (18); remodeling index = VA stenosis/VA reference (an index >1.05 indicates positive remodeling; other scores indicate nonpositive remodeling); degree of stenosis = (1 – LA stenosis/VA reference) × 100% (19).

To minimize the biasing of the results, one of the two radiologists (Y.T.) measured the VA stenosis, VA reference, LA stenosis, and LA reference again after 1 month.

Statistical analysis

SPSS 26.0 software (IBM Corp., Armonk, NY, USA) was used for statistical analysis. Measurement data are expressed as the mean ± standard deviation ($\bar{x} \pm s$) or as the median and interquartile range, and count data are expressed as percentages. Normality tests for quantitative data were performed using the Shapiro-Wilk test, while the two-sample *t*-test, nonparametric rank sum test, and chi-square test were used to compare the variability between plaque vulnerability parameters of the different WMH subgroups. Spearman correlation coefficient analysis was used to determine the correlation between different WMHs classifications and plaque parameters. The relationship between plaque characteristics on HR-MRI and WMHs were determined via binary logistic regression analysis, and variables with P<0.05 on univariate analysis were incorporated into multivariate logistic regression analysis. The degree of agreement

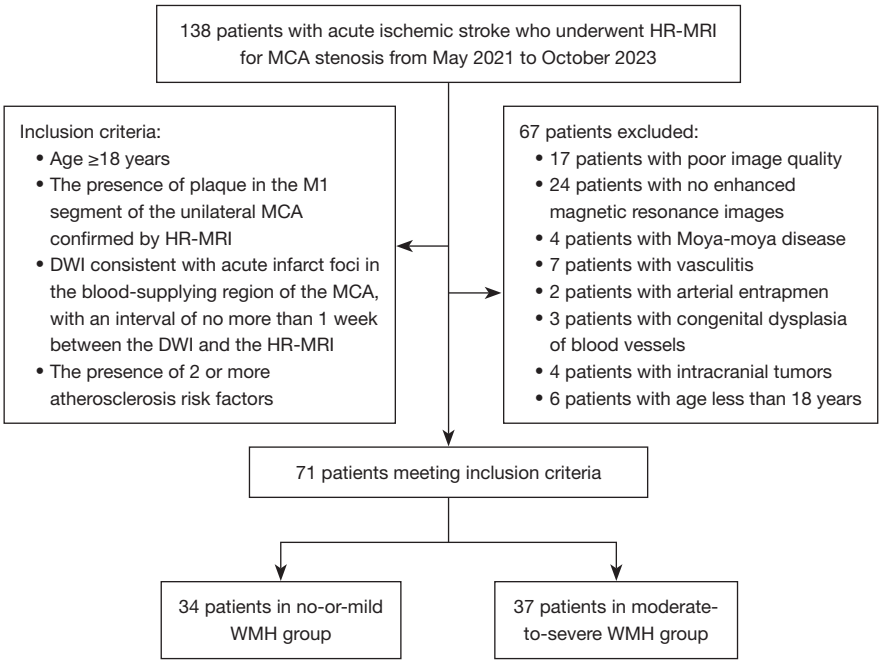

Figure 1 The flowchart of patient enrollment in this study. HR-MRI, high-resolution magnetic resonance imaging; MCA, middle cerebral artery; DWI, diffusion-weighted imaging; WMH, white matter hyperintensity.

between the radiologists in measuring area was evaluated using intragroup correlation coefficients (ICCs). ICC values less than 0.4 indicated poor consistency; 0.4–0.75, moderate consistency; and 0.75 s, good consistency. A two-tailed P value <0.05 was considered statistically significant.

Results

Basic information

A total of 138 patients who underwent HR-MRI from May 2021 to October 2023 were initially considered for this study, among whom 71 with acute ischemic stroke were enrolled according to the inclusion and exclusion criteria. A flowchart of patient inclusion can be seen in *Figure 1*. There were 34 cases (47.9%) in group 1 (no-or-mild WMHs) and 37 cases (52.1%) in group 2 (moderate-to-severe WMHs) (*Figures 2,3*). There were differences between the two groups in terms of gender, BMI, diabetes mellitus, dyslipidemia, history of smoking, and history of stroke or TIA, which were not statistically significant (all P values >0.05); however, there were significant differences in age (P=0.01) and proportion of hypertension (P=0.01). The clinical data of the patients in the two groups are shown in *Table 2* and *Figure 4*.

Comparison of plaque characteristics

Among the 71 patients enrolled, there were 20 (27.8%) cases of intraplaque hemorrhage, 22 (30.6%) cases of positive remodeling, 33 (45.8%) cases of wide distribution, and 14 (19.4%) cases of significant enhancement. There were no significant differences in LA stenosis, VA stenosis, LA reference, VA reference, stenosis degree, plaque load, or positive remodeling between group 1 and 2 (all P values >0.05). However, there were significant differences between the two groups in the proportion of intraplaque hemorrhage (P=0.01), the proportion of widely distributed plaque (P=0.02), and the proportion of significantly enhanced plaque (P=0.02) (*Figure 5*). In group 2, there was a greater proportion of widely distributed plaque (59.5%), intraplaque hemorrhage (40.5%), and significant enhancement (29.7%), as shown in *Table 3*.

Correlation analysis

Spearman correlation analysis showed that different degrees of WMHs were weakly positively correlated with age (r=0.300; P=0.01), hypertension (r=0.294; P=0.01), intraplaque hemorrhage (r=0.271; P=0.02), widely distributed plaque (r=0.287; P=0.01), and significantly enhanced plaque (r=0.262; P=0.02).

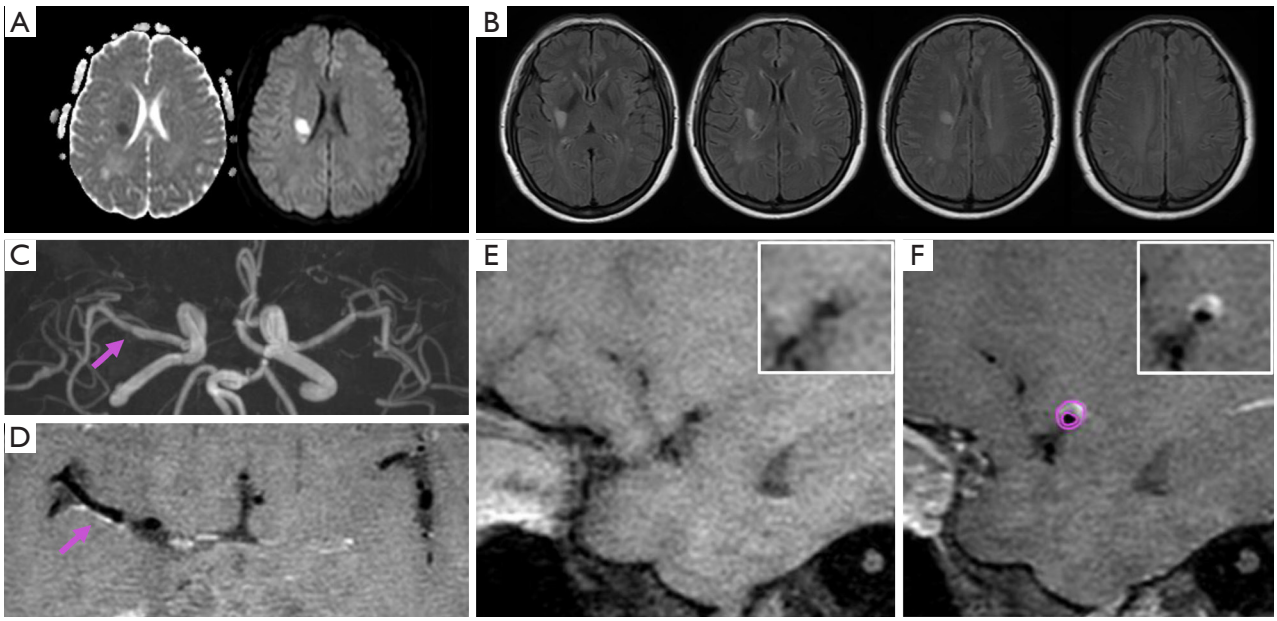

Figure 2 A female patient with mild white matter hyperintensities. The patient was a 55-year-old female and had experienced acute ischemic stroke. (A) The right basal ganglia region had restricted diffusion, with low signal in this region on the ADC map and a restricted high signal on the b=1,000 map. (B) A "hat-shaped" high signal in the anterior horns of the lateral ventricles bilaterally and a small punctate high signal scattered in the deep lateral ventricles visible on the head magnetic resonance T2 FLAIR image. (C) Reconstruction of the MIP image (arrow) showing mild stenosis in the M1 segment of the right middle cerebral artery. (D) Post-enhancement long-axis T1 VISTA image suggesting increased plaque signal (arrow) along the M1 vascular pathway. (E) Pre-enhancement and (F) post-enhancement short-axis T1 VISTA of the vasculature showing limited distribution of plaques and nonsignificant enhancement of the plaques; the purple circles outline the internal and external regions of interest. ADC, apparent diffusion coefficient; FLAIR, fluid-attenuated inversion recovery; MIP, maximum intensity projection; VISTA, volumetric isotropic turbo spin echo acquisition.

Logistic analysis

Age, hypertension, intraplaque hemorrhage, and significantly enhanced plaque were included in the multivariate logistic regression analysis, and the results showed that the independent risk factors for WMHs were age [odds ratio (OR) =1.095; 95% confidence interval (CI): 1.019–1.176; P=0.01] and intraplaque hemorrhage (OR =5.881; 95% CI: 1.466–23.592; P=0.01) (*Table 4*).

Consistency results

The consistency of measurement for VA stenosis, LA stenosis, VA reference, and LA reference of the two radiologists was good (*Table 5*).

Discussion

In this study, the plaque characteristics of stenotic vessels were measured with HR-MRI. The results showed that those with moderate or severe WMHs tended to be older, more hypertensive, and more prone to intraplaque hemorrhage and to have significantly enhanced and widely distributed plaques. Age, hypertension, plaque distribution, intraplaque hemorrhage, and significant enhancement were weakly correlated with WMH grading, among which age and intraplaque hemorrhage were independent risk factors for WMHs.

The possible mechanisms underlying the emergence of WMHs include endothelial dysfunction, chronic ischemia, blood-brain barrier (BBB) disruption, and impaired venous drainage. Atherosclerotic lesions are systemic inflammation that leads to increased permeability of the BBB, and BBB disruption is associated with the development of CSVD (20). With the rapid advancement of computer technology in recent years, new possibilities in MRI have emerged, including the accurate segmentation of the gray and white matter of the brain. These novel approaches

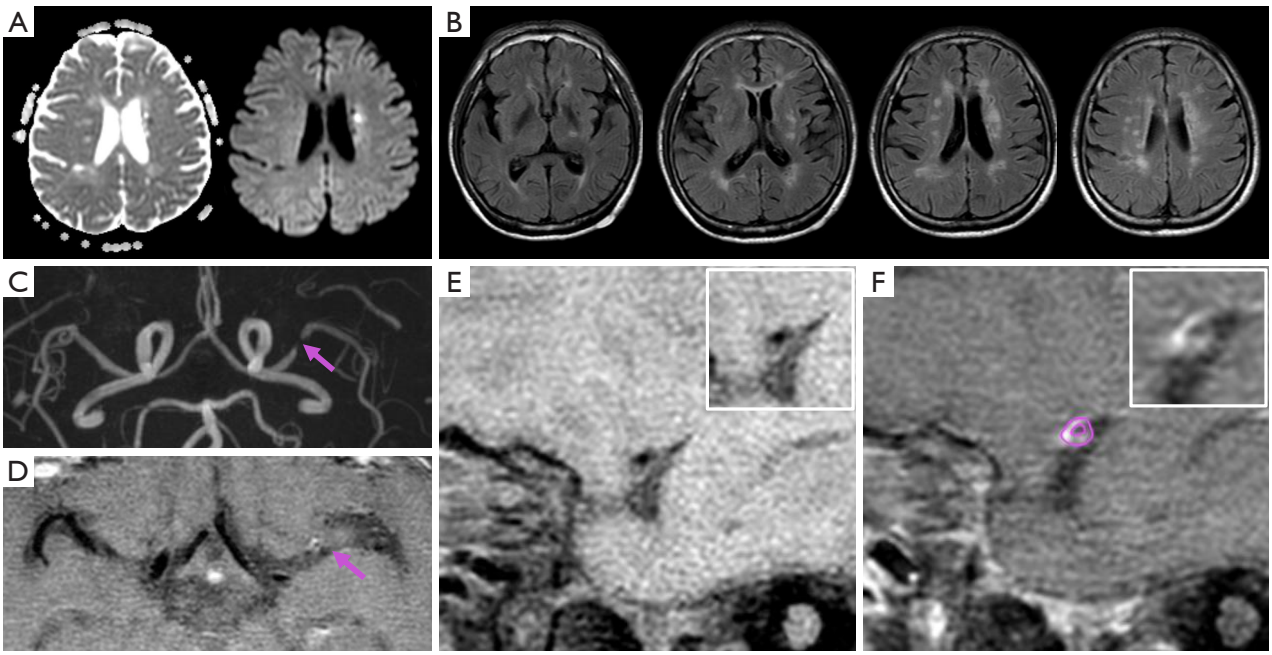

Figure 3 A patient with moderate white matter hyperintensities. The patient was a 65-year-old male who had experienced acute ischemic stroke. (A) The left lateral paraventricular diffusion appeared restricted, with low signal in this region on ADC map and restricted high signal on b=1,000 map. (B) Multiple, scattered distribution and patchy high signal in bilateral lateral ventricles and deep lateral ventricles visible on a head magnetic resonance MRI T2 FLAIR image. (C) 3D-TOF-MRA reconstructed MIP image showing restricted stenosis of the M1 segment of the left middle cerebral artery, with stenotic segments (arrow). (D) Enhanced vascular long-axis T1 VISTA map showing increased plaque signal (arrow) along the M1 vessel alignment. Widely distributed plaques and significant plaque enhancement visible in (E) pre-enhanced and (F) post-enhanced vessel short-axis T1 VISTA; the purple circles outline internal and external regions of interest. ADC, apparent diffusion coefficient; MRI, magnetic resonance imaging; FLAIR, fluid-attenuated inversion recovery; 3D-TOF-MRA, three-dimensional time-of-flight magnetic resonance angiography; MIP, maximum intensity projection; VISTA, volumetric isotropic turbo spin echo acquisition.

hold tremendous promise for advancing the field of neuroscience and have led to numerous landmark findings (21-23). Conventional imaging methods have limitations in resolution, which makes it difficult to image small blood vessels in the brain. However, with the help of computer-aided algorithms, it is possible to segment these vessels. This method enables us to visualize the course and number of blood vessels and is an important tool in clinical research (24-26). HR-MRI can suppress the blood signals flowing in large blood vessels, obtain images of static tissues such as the walls of large blood vessels, and display images of the short axis of large blood vessels. This method can be used to evaluate the morphology and composition of atherosclerotic plaques in large arteries and then to determine the degree of vulnerability of plaques, thus offering high diagnostic value (27). However, there are relatively few studies that have used HR-MRI to investigate the relationship between large atherosclerotic plaque image features and cerebral cerebellar vasculature, and exploring the correlation between plaque load, plaque distribution, intraplaque hemorrhage, positive remodeling, plaque enhancement, and WMHs is still a relatively immature field.

Age and hypertension were associated with WMHs

WMHs are usually detected during physical examination, and related studies have shown that age and hypertension are important factors for WMHs. Research has demonstrated that the incidence of CSVD is positively correlated with age. There is a higher detection rate of CSVD in the older adult population than in the young and middle-aged population, and the risk of occurrence increases two to three times for every 10-year increase in age (28). Elevated arterial blood pressure may directly

Table 2 Differences in basic clinical information between the two groups

Characteristic	No-or-mild WMHs (n=34)	Moderate-to-severe WMHs (n=37)	$t/F/\chi^2$	P value
Age (years)[1]	54.50 (14.00)	60.00 (10.00)	–2.512	0.01*
Gender (male)[2]	27 (79.4)	25 (67.5)	1.268[a]	0.26
BMI (kg/m^2)[3]	24.90±2.66	25.11±2.73	–0.335[b]	0.73
Hypertension[2]	16 (47.1)	28 (75.7)	6.157[a]	0.01*
Diabetes[2]	14 (41.2)	16 (43.2)	0.031[a]	0.86
Dyslipidemia[2]	17 (50.0)	26 (70.3)	3.048[a]	0.08
Smoking[2]	17 (50.0)	20 (54.1)	0.117[a]	0.73
Stroke/TIA history[2]	25 (73.5)	28 (75.7)	0.043	0.83
Blood homocysteine (mmol/L)[1]	12.45 (4.56)	11.88 (7.84)	–0.668	0.50
Total cholesterol (mmol/L)[1]	3.76 (1.56)	4.37 (1.92)	–1.738	0.08
Triglyceride (mmol/L)[1]	1.44 (0.93)	1.58 (0.71)	–0.086	0.93
High-density lipoprotein (mmol/L)[3]	1.09±0.24	1.10±0.29	–0.117[b]	0.90
Low-density lipoprotein (mmol/L)[1]	2.26 (1.45)	2.69 (1.36)	–1.767	0.07

[1], median (interquartile range); [2], numbers (%); [3], mean ± standard deviation. [a], the value of χ^2; [b], the value of *t*; *, P<0.05. TIA, transient ischemic attack; WMH, white matter hyperintensity.

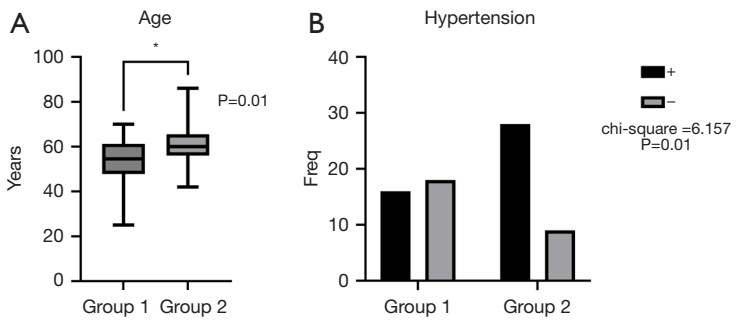

Figure 4 Differences in age and hypertension between the two groups. *, P<0.05. Group 1, no-or-mild white matter hyperintensities; Group 2, moderate-to-severe white matter hyperintensities.

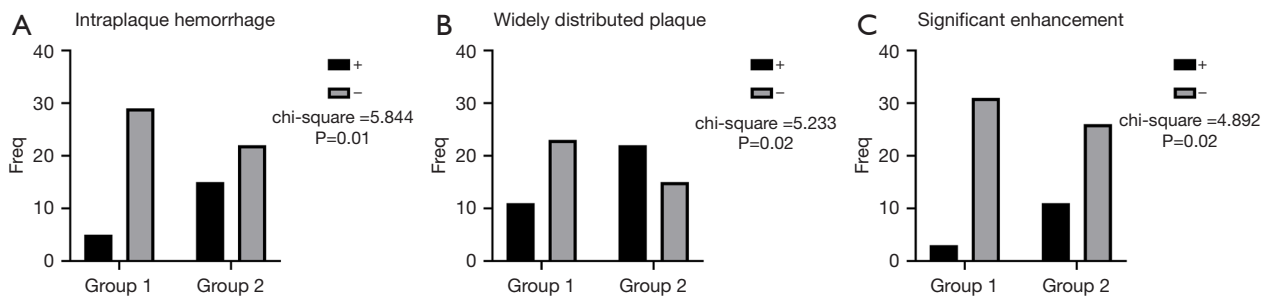

Figure 5 Differences in intraplaque hemorrhage, wide distribution, and significant enhancement between the two groups. Group 1, no-or-mild white matter hyperintensities; Group 2, moderate-to-severe white matter hyperintensities.

Table 3 Differences in plaque characteristics between the two groups

Characteristic	No-or-mild WMHs (n=34)	Moderate-to-severe WMHs (n=37)	$t/F/\chi^2$	P value
Stenotic vessel area (mm^2)[1]	8.82 (3.54)	10.23 (4.58)	–1.629	0.10
Stenotic lumen area (mm^2)[1]	1.88 (1.32)	2.27 (2.25)	–1.307	0.19
Reference vessel area (mm^2)[1]	9.84 (2.96)	11.20 (3.60)	–1.548	0.12
Reference lumen area (mm^2)[1]	4.45 (2.40)	5.20 (3.25)	–0.852	0.39
Plaque load (%)[1]	0.77 (0.16)	0.76 (0.15)	–0.829	0.40
Remodeling index[2]	0.85±0.22	0.89±0.23	–0.582[b]	0.56
Positive remodeling[3]	8 (23.5)	14 (37.8)	1.696[a]	0.19
Intraplaque hemorrhage[3]	5 (14.7)	15 (40.5)	5.844[a]	0.01*
Widely distributed plaque[3]	11 (32.4)	22 (59.5)	5.233[a]	0.02*
Stenosis degree (%)[1]	0.81 (0.13)	0.78 (0.17)	–0.742	0.45
Significantly enhanced plaque[3]	3 (8.8)	11 (29.7)	4.892[a]	0.02*

[1], median (interquartile range); [2], mean ± standard deviation; [3], numbers (%). [a], the value of χ^2; [b], the value of t; *, P<0.05. WMH, white matter hyperintensity.

Table 4 Logistic analysis of clinical data, plaque characteristics, and white matter hyperintensities

Characteristic	Univariate logistic regression analysis		Multivariate logistic regression analysis	
	OR (95% CI)	P value	OR (95% CI)	P value
Age	1.080 (1.020–1.144)	0.008*	1.095 (1.019–1.176)	0.01*
Hypertension	3.500 (1.276–9.597)	0.01*	2.395 (0.703–8.165)	0.16
Widely distributed plaque	3.067 (1.159–8.115)	0.02*	2.413 (0.748–7.784)	0.14
Intraplaque hemorrhage	3.955 (1.247–12.538)	0.02*	5.881 (1.466–23.592)	0.01*
Significantly enhanced plaque	4.372 (1.101–17.358)	0.03*	2.769 (0.516–14.866)	0.23

*, P<0.05; OR, odds ratio; CI, confidence interval.

Table 5 Intra- and interobserver agreement

Characteristic	Intraobserver agreement		Interobserver agreement	
	ICC	95% CI	ICC	95% CI
Stenotic vessel area	0.953	0.925–0.970	0.932	0.893–0.957
Stenotic lumen area	0.950	0.922–0.969	0.940	0.906–0.962
Reference vessel area	0.932	0.893–0.957	0.913	0.865–0.945
Reference lumen area	0.910	0.860–0.943	0.922	0.878–0.951

ICC, intragroup correlation coefficient; CI, confidence interval.

increase the intima-media shear force, thickening the vessel wall and leading to hypoperfusion in the blood-supplied area, with high pressure further disrupting the BBB and causing chronic endothelial injury. The moderate-and-severe WMH subgroup in this study was positively correlated with age and hypertension, which is consistent with the findings of previous studies showing that age and hypertension are important factors affecting WMHs

(29,30). This may be explained by the fact that older age and hypertension are associated with the formation of atherosclerotic plaques.

Intraplaque hemorrhage, plaque enhancement, and plaque distribution were associated with WMHs

Vulnerable plaques are unstable plaques typically characterized by imaging features such as thin or incomplete fibrous caps, large lipid cores, positive remodeling, intraplaque hemorrhage or thrombosis, neovascularization or plaque enhancement, and a large plaque load (31). Intraplaque neovascularization figures prominently in atherosclerotic plaque formation and arterial remodeling. Intraplaque neovascularization promotes inflammatory cell infiltration, fibrous cap rupture, and intraplaque hemorrhage, which leads to plaque instability, rupture, and dislodgement of the plaque to form microemboli, which is an important feature of plaque vulnerability. When an MR contrast agent is injected intravenously, the plaque is markedly enhanced due to massive inflammatory cell infiltration and increased endothelial cell permeability. Using contrast enhancement of intraplaque neovascularization and a semiquantitative visual grading scale, Wang *et al.* demonstrated that carotid intraplaque hemorrhage is independently associated with WMH exacerbation (32). Plaque enhancement in ischemic stroke varies by period. Yang *et al.* classified stroke according to the period of stroke onset into acute (<4 weeks), subacute (4–12 weeks), and chronic (>12 weeks) and after comparing the degree of plaque enhancement among the three groups, found that plaque enhancement was more pronounced in the acute period (33). Another study on intracranial atherosclerotic plaque enhancement reported a correlation between the asymmetry of deep WMHs and plaque enhancement (34). These findings cumulatively indicate that examining intraplaque hemorrhage is highly relevant to characterizing the changes in white matter.

The participants in our study had all experienced acute ischemic stroke, and the experimental results showed that the proportion of those with significant plaque enhancement was significantly higher in the moderate-and-severe WMH group than in the no-or-mild WMH group. This may be attributed to the increase in vascular permeability, which further damages the cerebral white matter.

Plaque distribution is thought to be associated with ischemic stroke, Zhu *et al.* explored the plaque characteristics of small subcortical infarcts and large subcortical infarcts in the MCA and found that the extent of plaque distribution was more restricted in the small-infarct group (35). Our experimental results suggest that wide plaque is associated with a more severe degree of WMH and that plaque with wide diffusion may represent intraplaque microvascular infiltration and active inflammation, all of which can lead to BBB disruption, resulting in irregularities and the mechanical vulnerability of the plaque surface.

Positive remodeling and plaque load were not associated with WMHs

Positive remodeling is a type of remodeling in which the wall expands outward due to altered plaque composition, continuous damage, and repair. Although this remodeling delays luminal stenosis, the accumulation of inflammatory cells leads to plaque instability and a greater susceptibility to rupture, which is closely related to the occurrence of stroke (5,36). Few studies have used HR-MRI alone to assess the relationship between positive remodeling and WMHs, and in our study, no correlation was found between positive remodeling and WMHs. This is likely because positive remodeling of the vessel wall usually occurs at the early stage of atherosclerotic plaque formation, and with the aggravation of the lesion to the advanced stage, the lumen of the vessel gradually narrows to become nonpositive remodeling. In our study, only the minority of participants were in the early stage of plaque formation, and a small portion of participants underwent HR-MRI; thus, no correlation could be found. In their study, Zwartbol *et al.* used the number of vascular lesions to reflect the intracranial atherosclerotic load and found that intracranial atherosclerotic load was associated with CSVD (37). In general, plaque load represents a morphological indicator of plaque-destabilizing factors, with a larger plaque load implying a larger plaque and a larger plaque implying a greater vulnerability to damage. Studies on plaque load and ischemic stroke are sparse, and the few findings that have been published are controversial (37-39). In a study using HR-MRI to study arterial remodeling in basilar artery stenosis, the remodeling pattern was found to be strongly associated with plaque load (40). A standardized vessel wall index was used to indicate plaque load, and no correlation between plaque load and WMHs was reported. Further research in this field is needed in the future.

Limitations

This study had several limitations which should be

addressed. First, the volume of patients we retrospectively collected was relatively small, resulting in limited experimental results. Moreover, we employed a single-center, cross-sectional design, and thus future multicenter longitudinal studies are needed to provide a dynamic and in-depth understanding of the relationship between vulnerable plaques and WMHs. Second, Fazekas grading as a visual scoring method is subjective and has low diagnostic efficacy, and subsequent studies should investigate the location, distribution, morphology, and volume of WMHs through direct myelin imaging or computer-assisted image segmentation. Finally, our assessment of plaque enhancement was qualitative and not quantitative. In subsequent research, an enhancement index or enhancement rate might be considered to more accurately evaluate plaque enhancement.

Conclusions

We identified intraplaque hemorrhage in the MCA via HR-MRI technique and experimentally demonstrated that age, hypertension, intraplaque hemorrhage, widespread plaque distribution, and significant plaque enhancement were associated with the severity of WMHs. Older age and intraplaque hemorrhage are important factors associated with the alteration of WMHs, further confirming that vulnerable plaques in the MCA are linked to the white matter alterations in the brain.

Acknowledgments

Funding: This research was supported by the Health Commission Foundation of Heilongjiang Province of China (No. 2020-099).

Footnote

Reporting Checklist: The authors have completed the STROBE reporting checklist. Available at https://qims.amegroups.com/article/view/10.21037/qims-23-1856/rc

Conflicts of Interest: All authors have completed the ICMJE uniform disclosure form (available at https://qims.amegroups.com/article/view/10.21037/qims-23-1856/coif). J.L. is an employee of Philips Healthcare (Beijing, China). The other authors have no conflicts of interest to declare.

Ethical Statement: The authors are accountable for all aspects of the work in ensuring that questions related to the accuracy or integrity of any part of the work are appropriately investigated and resolved. This study was conducted in accordance with the Declaration of Helsinki (as revised in 2013) and was approved by the institutional review board of the First Hospital of Harbin Medical University (No. 2023JS24). The requirement of individual consent for this retrospective analysis was waived.

References

1. Delano-Wood L, Bondi MW, Sacco J, Abeles N, Jak AJ, Libon DJ, Bozoki A. Heterogeneity in mild cognitive impairment: differences in neuropsychological profile and associated white matter lesion pathology. J Int Neuropsychol Soc 2009;15:906-14.
2. Swardfager W, Cogo-Moreira H, Masellis M, Ramirez J, Herrmann N, Edwards JD, et al. The effect of white matter hyperintensities on verbal memory: Mediation by temporal lobe atrophy. Neurology 2018;90:e673-82.
3. Lindenholz A, de Bresser J, van der Kolk AG, van der Worp HB, Witkamp TD, Hendrikse J, van der Schaaf IC. Intracranial Atherosclerotic Burden and Cerebral Parenchymal Changes at 7T MRI in Patients With Transient Ischemic Attack or Ischemic Stroke. Front Neurol 2021;12:637556.
4. Li S, Song X, Hu Q, Zhao J, Du H, Yan Y, Wang G, Chen X, Wang Q. Association of Plaque Features with Infarct Patterns in Patients with Acutely Symptomatic Middle Cerebral Artery Atherosclerotic Disease. J Stroke Cerebrovasc Dis 2021;30:105724.
5. Zhang DF, Chen YC, Chen H, Zhang WD, Sun J, Mao CN, Su W, Wang P, Yin X. A High-Resolution MRI Study of Relationship between Remodeling Patterns and Ischemic Stroke in Patients with Atherosclerotic Middle Cerebral Artery Stenosis. Front Aging Neurosci 2017;9:140.
6. Song JW, Pavlou A, Burke MP, Shou H, Atsina KB, Xiao

J, Loevner LA, Mankoff D, Fan Z, Kasner SE. Imaging endpoints of intracranial atherosclerosis using vessel wall MR imaging: a systematic review. Neuroradiology 2021;63:847-56.
7. Zerna C, Yu AYX, Modi J, Patel SK, Coulter JI, Smith EE, Coutts SB. Association of White Matter Hyperintensities With Short-Term Outcomes in Patients With Minor Cerebrovascular Events. Stroke 2018;49:919-23.
8. Ammirati E, Moroni F, Magnoni M, Rocca MA, Anzalone N, Cacciaguerra L, Di Terlizzi S, Villa C, Sizzano F, Palini A, Scotti I, Besana F, Spagnolo P, Rimoldi OE, Chiesa R, Falini A, Filippi M, Camici PG. Progression of brain white matter hyperintensities in asymptomatic patients with carotid atherosclerotic plaques and no indication for revascularization. Atherosclerosis 2019;287:171-8.
9. Berman SE, Wang X, Mitchell CC, Kundu B, Jackson DC, Wilbrand SM, Varghese T, Hermann BP, Rowley HA, Johnson SC, Dempsey RJ. The relationship between carotid artery plaque stability and white matter ischemic injury. Neuroimage Clin 2015;9:216-22.
10. Zhang D, Wang M, Wu L, Zhao Y, Wang S, Yin X, Wu X. Assessing the characteristics and diagnostic value of plaques for patients with acute stroke using high-resolution magnetic resonance imaging. Quant Imaging Med Surg 2022;12:1529-38.
11. Zhong T, Qi Y, Li R, Zhou H, Ran B, Wang J, Cai Z. Contribution of intracranial artery stenosis to white matter hyperintensities progression in elderly Chinese patients: A 3-year retrospective longitudinal study. Front Neurol 2022;13:922320.
12. Wang J, Zhang S, Lu J, Qi P, Hu S, Yang X, Chen K, Wang D. High-Resolution MR for Follow-Up of Intracranial Steno-Occlusive Disease Treated by Endovascular Treatment. Front Neurol 2021;12:706645.
13. Fazekas F, Chawluk JB, Alavi A, Hurtig HI, Zimmerman RA. MR signal abnormalities at 1.5 T in Alzheimer's dementia and normal aging. AJR Am J Roentgenol 1987;149:351-6.
14. van Straaten EC, Fazekas F, Rostrup E, Scheltens P, Schmidt R, Pantoni L, Inzitari D, Waldemar G, Erkinjuntti T, Mäntylä R, Wahlund LO, Barkhof F; . Impact of white matter hyperintensities scoring method on correlations with clinical data: the LADIS study. Stroke 2006;37:836-40.
15. Wang J, Börnert P, Zhao H, Hippe DS, Zhao X, Balu N, Ferguson MS, Hatsukami TS, Xu J, Yuan C, Kerwin WS. Simultaneous noncontrast angiography and intraplaque hemorrhage (SNAP) imaging for carotid atherosclerotic disease evaluation. Magn Reson Med 2013;69:337-45.
16. Qiao Y, Zeiler SR, Mirbagheri S, Leigh R, Urrutia V, Wityk R, Wasserman BA. Intracranial plaque enhancement in patients with cerebrovascular events on high-spatial-resolution MR images. Radiology 2014;271:534-42.
17. Xu WH, Li ML, Gao S, Ni J, Zhou LX, Yao M, Peng B, Feng F, Jin ZY, Cui LY. Plaque distribution of stenotic middle cerebral artery and its clinical relevance. Stroke 2011;42:2957-9.
18. Du H, Li J, Yang W, Bos D, Zheng L, Wong LKS, Leung TW, Chen X. Intracranial Arterial Calcification and Intracranial Atherosclerosis: Close but Different. Front Neurol 2022;13:799429.
19. Li J, Wu H, Hang H, Sun B, Zhao H, Chen Z, Zhou Y, Xu J, Chen J, Zhou D, Zhao X, Yuan C. Carotid vulnerable plaque coexisting with cerebral small vessel disease and acute ischemic stroke: a Chinese Atherosclerosis Risk Evaluation study. Eur Radiol 2022;32:6080-9.
20. Banerjee C, Chimowitz MI. Stroke Caused by Atherosclerosis of the Major Intracranial Arteries. Circ Res 2017;120:502-13.
21. Jia Z, Zhu H, Zhu J, Ma P. Two-Branch network for brain tumor segmentation using attention mechanism and super-resolution reconstruction. Comput Biol Med 2023;157:106751.
22. Sedaghat S, Jang H, Ma Y, Afsahi AM, Reichardt B, Corey-Bloom J, Du J. Clinical evaluation of white matter lesions on 3D inversion recovery ultrashort echo time MRI in multiple sclerosis. Quant Imaging Med Surg 2023;13:4171-80.
23. Sedaghat S, Jang H, Athertya JS, Groezinger M, Corey-Bloom J, Du J. The signal intensity variation of multiple sclerosis (MS) lesions on magnetic resonance imaging (MRI) as a potential biomarker for patients' disability: A feasibility study. Front Neurosci 2023;17:1145251.
24. Ryu J, Rehman MU, Nizami IF, Chong KT. SegR-Net: A deep learning framework with multi-scale feature fusion for robust retinal vessel segmentation. Comput Biol Med 2023;163:107132.
25. Zheng C, Li H, Ge Y, He Y, Yi Y, Zhu M, Sun H, Kong J. Retinal vessel segmentation based on multi-scale feature and style transfer. Math Biosci Eng 2024;21:49-74.
26. Rehman MU, Ryu J, Nizami IF, Chong KT. RAAGR2-Net: A brain tumor segmentation network using parallel processing of multiple spatial frames. Comput Biol Med 2023;152:106426.
27. Mandell DM, Mossa-Basha M, Qiao Y, Hess CP, Hui F, Matouk C, Johnson MH, Daemen MJ, Vossough A,

Edjlali M, Saloner D, Ansari SA, Wasserman BA, Mikulis DJ; Vessel Wall Imaging Study Group of the American Society of Neuroradiology. Intracranial Vessel Wall MRI: Principles and Expert Consensus Recommendations of the American Society of Neuroradiology. AJNR Am J Neuroradiol 2017;38:218-29.
28. Fang M, Feng C, Xu Y, Hua T, Jin AP, Liu XY. Microbleeds and silent brain infarctions are differently associated with cognitive dysfunction in patients with advanced periventricular leukoaraiosis. Int J Med Sci 2013;10:1307-13.
29. Keller JA, Kant IMJ, Slooter AJC, van Montfort SJT, van Buchem MA, van Osch MJP, Hendrikse J, de Bresser J. Different cardiovascular risk factors are related to distinct white matter hyperintensity MRI phenotypes in older adults. Neuroimage Clin 2022;35:103131.
30. Nam KW, Kwon HM, Jeong HY, Park JH, Kim SH, Jeong SM, Yoo TG, Kim S. Cerebral white matter hyperintensity is associated with intracranial atherosclerosis in a healthy population. Atherosclerosis 2017;265:179-83.
31. Naghavi M, Libby P, Falk E, Casscells SW, Litovsky S, Rumberger J, et al. From vulnerable plaque to vulnerable patient: a call for new definitions and risk assessment strategies: Part I. Circulation 2003;108:1664-72.
32. Wang Y, Jiang C, Huang H, Liu N, Wang Y, Chen Z, Liang S, Wu M, Jiang Y, Wang X, Zhou T, Chen H, Zhang L, Li H. Correlation of Cerebral White Matter Lesions with Carotid Intraplaque Neovascularization assessed by Contrast-enhanced Ultrasound. J Stroke Cerebrovasc Dis 2020;29:104928.
33. Yang WJ, Abrigo J, Soo YO, Wong S, Wong KS, Leung TW, Chu WC, Chen XY. Regression of Plaque Enhancement Within Symptomatic Middle Cerebral Artery Atherosclerosis: A High-Resolution MRI Study. Front Neurol 2020;11:755.
34. Ni L, Zhou F, Qing Z, Zhang X, Li M, Zhu B, Zhang B, Xu Y. The Asymmetry of White Matter Hyperintensity Burden Between Hemispheres Is Associated With Intracranial Atherosclerotic Plaque Enhancement Grade. Front Aging Neurosci 2020;12:163.
35. Zhu T, Ren L, Zhang L, Shao Y, Wan L, Li Y, Liang D, Zheng H, Liu X, Zhang N. Comparison of plaque characteristics of small and large subcortical infarctions in the middle cerebral artery territory using high-resolution magnetic resonance vessel wall imaging. Quant Imaging Med Surg 2021;11:57-66.
36. Cilla M, Peña E, Martínez MA, Kelly DJ. Comparison of the vulnerability risk for positive versus negative atheroma plaque morphology. J Biomech 2013;46:1248-54.
37. Zwartbol MH, van der Kolk AG, Kuijf HJ, Witkamp TD, Ghaznawi R, Hendrikse J, Geerlings MI; UCC-SMART Study Group. Intracranial vessel wall lesions on 7T MRI and MRI features of cerebral small vessel disease: The SMART-MR study. J Cereb Blood Flow Metab 2021;41:1219-28.
38. Lu M, Zhang L, Yuan F, Peng P, Zhang H, Liu S, He Y, Cai J, Zhao X. Comparison of carotid atherosclerotic plaque characteristics between symptomatic patients with transient ischemic attack and stroke using high-resolution magnetic resonance imaging. BMC Cardiovasc Disord 2022;22:190.
39. Elhfnawy AM, Volkmann J, Schliesser M, Fluri F. Corrigendum: Are Cerebral White Matter Lesions Related to the Presence of Bilateral Internal Carotid Artery Stenosis or to the Length of Stenosis Among Patients With Ischemic Cerebrovascular Events? Front Neurol 2019;10:1058.
40. Luo J, Bai X, Tian Q, Li L, Wang T, Xu R, Gong H, Wang Y, Chen Y, Gao P, Chen J, Yang B, Ma Y, Dmytriw AA, Jiao L. Patterns and implications of artery remodeling based on high-resolution vessel wall imaging in symptomatic severe basilar artery stenosis. Quant Imaging Med Surg 2023;13:2098-108.

Cite this article as: Li J, Tian Y, Shi Y, Cui Y, Lian J, Liu P. Association of vulnerable plaques with white matter hyperintensities on high-resolution magnetic resonance imaging. Quant Imaging Med Surg 2024;14(5):3606-3618. doi: 10.21037/qims-23-1856

